ACS APPLIED MATERIALS & INTERFACES

Research Article

www.acsami.org

A Nonconjugated Bridge in Dimer-Sensitized Solar Cells Retards Charge Recombination without Decreasing Charge Injection Efficiency

Kenji Sunahara,[†] Matthew J. Griffith,[§] Takayuki Uchiyama,[†] Pawel Wagner,[§] David L. Officer,[§] Gordon G. Wallace,[§] Attila J. Mozer,*[,§] and Shogo Mori*[,†]

[†]Division of Chemistry and Materials, Faculty of Textile Science and Technology, Shinshu University, Ueda, Nagano 386-8567, Japan

[§]ARC Centre of Excellence for Electromaterials Science and Intelligent Polymer Research Institute, University of Wollongong, Innovation Campus, Squires Way, Fairy Meadow, New South Wales 2519, Australia

Supporting Information

ABSTRACT: Dye sensitized solar cells (DSSCs) employing a dimer porphyrin, which was synthesised with two porphyrin units connected without conjugation, have shown that both porphyrin components can contribute to photocurrent generation, that is, more than 50 % internal quantum efficiency. In addition, the open-circuit voltage (V_{oc}) of the DSSCs was higher than that of DSSCs using monomer porphyrins. In this paper, we first optimized cell structure and fabrication conditions. We obtained more than 80% incident photon to current conversion efficiency from the dimer porphyrin sensitized DSSCs and higher V_{oc} and energy conversion efficiency than monomer porphyrin sensitized solar cells. To examine the origin of the higher V_{oc}, we measured electron lifetime in the DSSCs with various conditions, and found that the dimer system increased the electron lifetime by improving the steric blocking effect of the dye layer, whilst the lack of a conjugated linker prevents an increase in the attractive force between conjugated sensitizers and the acceptor species in the electrolyte. The results support a hypothesis; dispersion force is one of the factors influencing the electron lifetime in DSSCs.

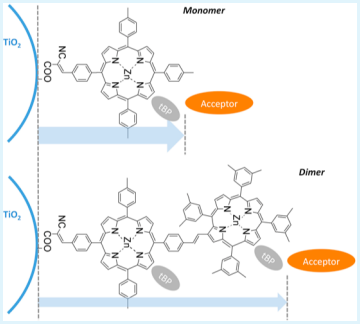

KEYWORDS: *electron injection, recombination, electron lifetime, porphyrin, dispersion force*

INTRODUCTION

Sensitization of nanocrystalline oxides with organic and inorganic light-harvesting compounds is a promising pathway for the development of low-cost renewable energy conversion devices.[1] One of the challenges in the development of highly efficient dye-sensitized solar cells (DSSCs) is to retard charge recombination.[2] Although the recombination process is dependent on a range of factors, one of the key materials controlling this reaction has been shown to be the sensitizers themselves.[3,4] We have previously reported that the open circuit voltage (V_{oc}) of porphyrin-based DSSCs is typically lower than those of other efficient ruthenium complex dyes.[5] This was attributed to a short lifetime of TiO_2 electrons primarily recombining with triiodide (I_3^-) ions, the acceptor species in the electrolyte. This recombination reaction has been found to be a general problem for many organic sensitizers limiting their open circuit voltage.[6,7] The major reason for this lower photovoltage is that adsorption of sensitizers on the TiO_2 surface acts to facilitate charge recombination with the redox mediator. It has been proposed that one origin of this enhanced recombination is the dispersion force on the sensitizer attracting the acceptor species to the TiO_2 surface region and increasing the probability of reverse charge transfer.[8] Because this dispersion force scales with the length of the π conjugation unit,[9] sensitizers with a smaller size are desired to minimize recombination. However, such dyes have narrow absorption spectra, which prevent their use as efficient sensitizers in solar cells. Most previous attempts to decrease the charge recombination in DSSCs have therefore concentrated on insulating the TiO_2 with surface treatments,[10−12] small co-adsorber molecules,[13−16] or small co-adsorber with alkyl chains,[17] or to add alkyl chains to sensitizers to prevent the approach of the electron acceptor species to the TiO_2 surface.[18−20] Recently, such strategies were incorporated into the design of a porphyrin sensitizer to produce a record power conversion efficiency of 12.1%.[21]

Recently, attention has been given to dimer sensitizers. One motivation to apply dimers for DSSCs is to extend the absorption spectrum into the infrared. For this purpose, two molecules are connected with conjugated linker. The other motivation is to increase light absorption coefficients of sensitizers. For this case, molecules are connected using non-conjugated bridge. By increasing the coefficients, the thickness of the porous electrodes can be reduced. Table 1 summarizes recently published data for dimer sensitized solar cells.[22−26] As expected, using conjugated linker results in the extension of

Received: July 25, 2013
Accepted: October 1, 2013
Published: November 4, 2013

Table 1. Summary of Reported Performance of DSSCs Employing Dimer Sensitizers

authors	dye	IPCE$_{max}$ (%)	IPCE onset (nm)	J_{sc} (mA cm^{-2})	V_{oc} (mV)	efficiency	ref
Warnan et. al.	dimer	40	745	11.6	535	4.6	22
	monomer	30	730	9.25	545	3.6	
Park et. al	dimer	40-50	700	10.9	600	4.2	23
			no monomer data reported				
Wu et. al	dimer	30	900	9.66	680	4.7	24
	monomer 1	80	650	16.5	734	5.8	
	monomer 2	80	720	16.8	758	8.8	
Mai et. al	dimer	70	710	12.9	650	5.2	25
	monomer	60-70	680	10.9	710	5.1	
Liu et. al	dimer	60	850	14.3	550	5.2	26
			no monomer data reported				

absorption spectrum to longer wavelength, while it seems to result in the decrease of V_{oc}. On the other hand, dimer sensitizers using non-conjugated linker showed higher V_{oc} than monomer sensitizers. If the blocking effect of dye layers dominates the process of the charge recombination, employing dimer is always expected to result in the higher V_{oc} because of their larger molecular size. However, the data on Table 1 show that it is not always the case. If dispersion force affects the charge recombination and the effect can compete with the blocking effect, then the results on Table 1 would be more easily rationalized. On other hand, the dispersion force has not been accepted widely as one of the factors influencing the recombination. One of the aims of this paper is to examine the role of dispersion force in charge recombination by using a nonconjugated bridge in dimer-sensitized solar cells.

EXPERIMENTAL SECTION

Materials. Figure 1 shows the structure of dyes employed in this study. Porphyrin dyes **P12** (5,10,15,20-Tetra(3,5-dimethylphenyl)-2-(2-(4-carboxylphenyl)ethenyl)porphyrinato zinc(II)), **P199** ((5,10,15-tri(4-methylphenyl)-20-(4-(2-cyano-2-carboxylethenylphenyl)-porphyrinato zinc(II)), and dimer **P10** were prepared as previously reported.[27]

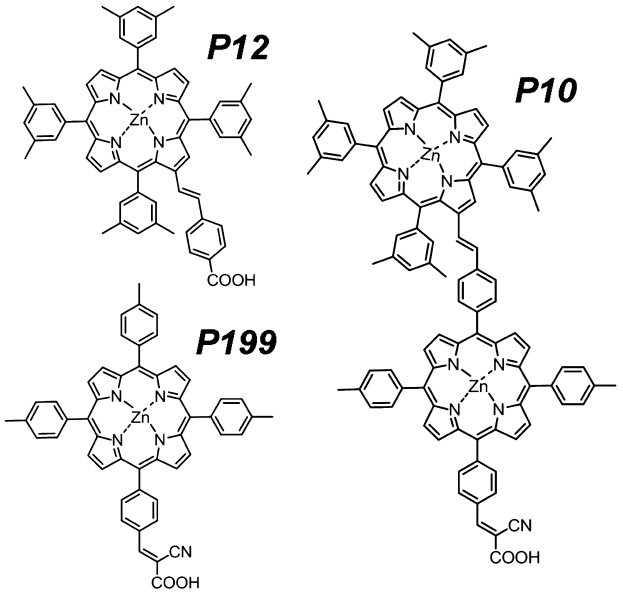

Figure 1. Chemical structures of porphyrin dyes **P10**, **P12**, **P199** employed in this study.

DSSC Fabrication. TiO_2 films were prepared on fluorine-doped tin oxide (FTO) substrates (Nippon Sheet Glass, $R_s \leq 9.5\ \Omega\ sq^{-1}$) using a doctor-blade technique and were sintered at 550°C for 30 minutes in air. DSSCs for high efficiency were prepared with a TiO_2 nano-particle paste from Sumitomo Osaka Cement Co. Ltd for a transparent layer and with a 400 nm TiO_2 particles (CCIC, Japan) for a scattering layer. Thickness of TiO_2 electrode, dye bath immersion time, and concentration of chenodeoxycholic acid (CDCA) were varied. DSSCs for lifetime measurements were prepared using around 5.4 μm transparent TiO_2 layer (Nanoxide-T, Solaronix) without scattering layer. Dye sensitization was achieved by immersion of TiO_2 films at around 80 °C into 0.2 mM or 0.02 mM ethanolic solutions of porphyrin dyes without CDCA and leaving at room temperature for 2 h or 30 min, respectively. Sandwich-type DSSCs were assembled using a thermal adhesive film and Pt-sputtered FTO-glass counter electrodes. Electrolyte solutions of varying composition were injected between the electrodes to complete devices. Electrolyte compositions employed in this study included:

Ia, 0.6 M 1,2-dimethyl-3-propylimidazolium (DMPImI), 0.5 M 4-tert-butylpyridine (tBP), 0.1 M LiI and 0.05 M I_2 in acetonitrile
Ib, 0.6 M 1-butyl-2-methyl-3-propylimidazolium (BMPImI), 0.5 M 4-tert-butylpyridine (tBP), 0.1 M LiI and 0.05 M I_2 in acetonitrile
II, 0.7 M BMPImI, 0.3 M tBP and 0.05 M I_2 in acetonitrile
III, 0.7 M DMPImI and 0.05 M I_2 in acetonitrile

DSSC Characterization. Current−voltage curves were recorded using a Keithley 2400 source measure unit with a simulated 100 mW cm^{-2} air mass AM 1.5 light source (YSS-100A, Yamashita Denso).

Electron Lifetime and Diffusion Coefficient Measurements. Electron lifetimes and diffusion coefficients were determined using stepped light-induced measurements of photocurrent and photovoltage transients (SLIM-PCV).[28] Measurements were performed using a 635 nm diode laser illuminating the entire DSSC active area. Photocurrent and photovoltage transients were induced by the small stepwise (≤10%) change of the laser intensity, controlled by a PC using a digital-to-analogue converter. Induced transients were measured by a fast multimeter (AD7461A, Advantest). Electron densities at each laser illumination intensities were determined by a charge extraction method in which the light source is switched off at the same time the DSSC is switched from open to short circuit.[29] The resulting current was integrated, with the electron density calculated from the amount of charge extracted.

RESULTS AND DISCUSSION

Optimizing Device Fabrication Conditions for Dimer-Sensitized Solar Cells. First, we checked the effect of dye bath concentration and immersion time on solar cells performance (Figures S1 and S2 in the Supporting Information) using electrolyte **Ia**. With both concentration and time, the values of J_{sc} were increased for the dimer and monomer sensitized solar cells, and further increase resulted in

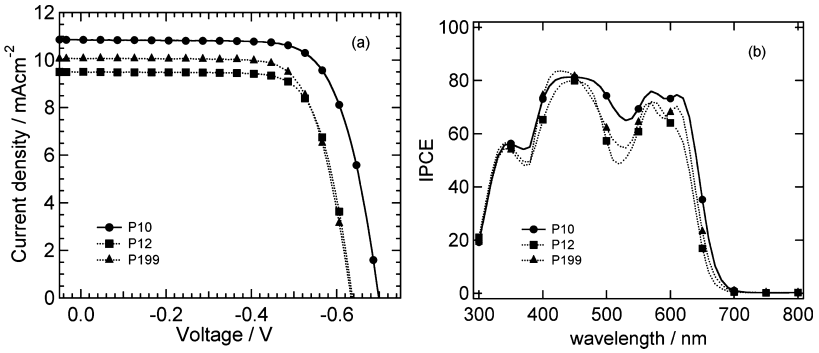

Figure 2. (a) $I-V$ curves and (b) IPCE of the optimized DSSCs using dimer (P10) and monomers (P12 and P199). The values of efficiency were 5.5 % (P10), 4.5% (P12), and 4.6% (P199).

the decrease in the values of J_{sc}. The decreased J_{sc} could be due to an undesired interaction among adsorbed dyes. Secondly, we examined the effect of co-adsorbent and immersion time. The concentration of dye was fixed and electrolyte **Ia** was employed. Table S1 in the Supporting Information summarizes the performance. The addition of CDCA increased the J_{sc} for both DSSCs using dimer and monomer. However, longer immersion time again resulted in the decrease of the J_{sc}. The concentration ratio of CDCA to dye was varied and 10:1 ratio was found to give the highest J_{sc}. The addition of scattering layer increased the J_{sc} by 20%. The thickness of the transparent layer was varied between 3.5 and 5.6 μm, and comparable values were obtained from 4.8 and 5.6 μm, suggesting the optimal thickness exists around 5 μm. The DSSCs using the dimer always showed higher values of V_{oc} than those of DSSCs using monomers. Figure 2 shows the $I-V$ curves and IPCE of the optimized DSSCs using dimer and monomers. Note that the IPCE spectra of the dimer and monomer cells were similar because the non-conjugated bridge of the dimer blocked the extension of molecular orbitals between the two porphyrin cores. Both the dimer and monomer DSSCs showed more than 80 % IPCE while the dimer DSSCs showed higher values of V_{oc}. The dimer DSSCs resulted in 5.5 % energy conversion efficiency, and the value was higher than those of the monomer DSSCs. The trend of the V_{oc} was the same to what we reported previously.[27] Comparable values of J_{sc} from both dimer and monomer DSSCs at optimized cells are expected because the range of absorption spectrum was the same. However, we note that more than 80% IPCE from the dimer DSSCs was hardly expected because the dimer was made by connecting two monomers having similar LUMO levels and the bridge was not conjugated. We have shown previously that both the monomer and dimer examined here suffer from sub-nanosecond charge recombination.[27] Thus, the increased IPCE using CDCA is probably caused by the retardation of the fast recombination with dye cation.

Electron Lifetime in DSSCs. In previous section, whereas the cell fabrication conditions were varied, the values of the V_{oc} from the dimer DSSCs were always higher than the values from the monomer DSSCs. The electron lifetime in the DSSCs were also measured, showing the electron lifetime in the dimer DSSCs always showed longer values regardless of the co-adsorption of CDCA and the addition of the scattering layer (see Figures S3 and S4 in the Supporting Information). To examine the origin of the longer electron lifetime, we compared here the electron lifetime in the DSSCs with various electrolyte conditions and different amount of dyes. To simplify the system, we employed cells without scattering layer and CDCA. The performance of the DSSCs employing electrolyte ***Ia*** without scattering layer and CDCA are shown in Table S2 and Figure S5 in the Supporting Information, and the trend was the same with the $I-V$ curves in Figure 2.

Electron lifetimes and diffusion coefficients for DSSCs prepared using the monomer and dimer porphyrin sensitizers are shown in Figure 3. Measurements were performed 3 times,

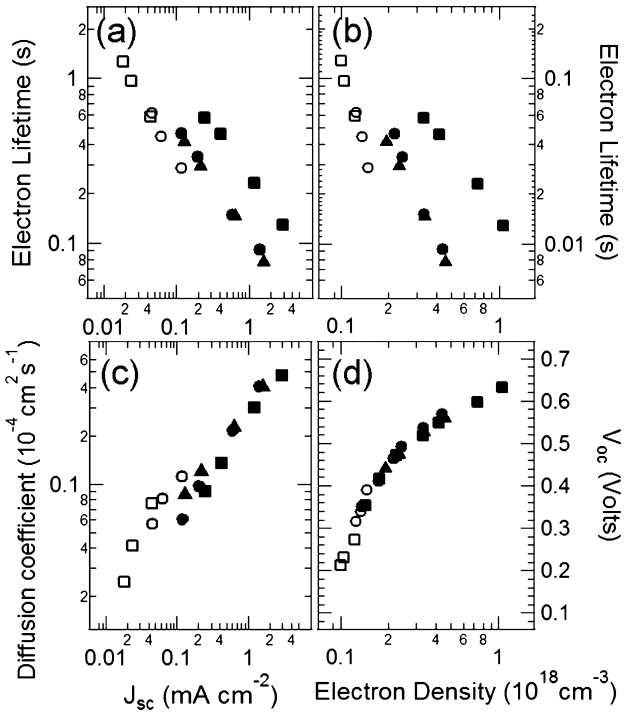

Figure 3. Electron lifetime versus (a) J_{sc}, or (b) electron density; electron diffusion coefficient versus (c) J_{sc}, and (d) V_{oc} versus electron density for DSSCs prepared with **P199** (circles), **P12** (triangles) and **P10** (squares). Measurements using reduced dye surface concentrations of **P199** (open circles) and **P10** (open squares) are also shown.

with the error in the resultant data points found to be less than 30 % of the values. At a matched electron density of 6×10^{17} cm^{-3}, the lifetime of dimer DSSCs was found to be higher than that of both monoporphyrins by an order of magnitude. The increased electron lifetime using the dimer may originate from slower electron transport within the TiO_2 in a trap-controlled recombination mechanism.[30] Figure 3c shows that there are

only minimal differences observed in the diffusion coefficients of DSSCs constructed from each dye system when plotted as a function of J_{sc}. This result indicates that variation in the charge transport is not the main origin of the increased lifetime for the dimer DSSCs. The plots of V_{oc} versus electron density in the TiO_2 film displayed no differences in either the slope or the y-intercept for DSSCs employing any of the three dyes (Figure 3d). This result demonstrates that the density of trap states[31] and the TiO_2 conduction band-edge potential (E_{CB}) are nearly identical for DSSCs prepared using porphyrin dyes **P199**, **P12**, and **P10**. The improved device V_{oc} observed in the dimer DSSCs is due to an increased electron density in the TiO_2 film caused by the increased electron lifetime.

Previous studies have proposed that the following three parameters are the major factors which influence the TiO_2 electron–I_3^- recombination reaction: (i) a steric blocking effect that reduces the concentration of I_3^- at the interface of dye-covered TiO_2 by physically blocking its approach;[6,32] (ii) an increased I_3^- concentration at the TiO_2 interface due to electrostatic forces, for example, attraction of the negatively charged acceptor species in the presence of partial charges on the dye molecules;[6] and (iii) an increased I_3^- concentration at the TiO_2 interface due to dispersion forces, for example, attraction of the acceptor species to the highly polarisable π-conjugated segments of dyes.[8] To distinguish between these causes and to gain further insights into the origin of the longer electron lifetime observed for the dimer DSSCs, the composition of the redox electrolyte was varied. In addition to the measurements performed with the standard composition of electrolyte **Ia**, DSSCs were also prepared using an electrolyte without LiI (0.7 M BMImI, 0.3 M tBP, 0.05 M I_2 in acetonitrile, referred to as electrolyte **II**) and without LiI and tBP (0.7 M DMPImI, 0.05 M I_2 in acetonitrile, referred to as electrolyte **III**). The Li^+ and tBP concentrations were varied because such species are known to have an influence on the charge recombination kinetics in DSSCs.[33−35] Furthermore, lithium cation has also been reported to interact with dye molecules,[36] and could therefore impact the recombination kinetics in the dimer DSSCs and monomer DSSCs differently. Photovoltaic performances for DSSCs containing each of these electrolytes are shown in Table S2 in the Supporting Information. It should be noted that we have ascertained that varying the cation from BMImI to DMPImI makes very little difference to the photovoltaic performance (see electrolytes **Ia** and **Ib** in Table S2 in the Supporting Information), charge transport and recombination dynamics (data not shown). They can therefore be used interchangeably in electrolytes **II** and **III**.

Figure 4 shows the electron lifetime for all dyes measured for DSSCs containing electrolytes **II** and **III**. For DSSCs with electrolyte **II**, the trend in the electron lifetime appears to be the same as electrolyte **I**, with the dimer DSSCs exhibiting a longer lifetime than the monomer DSSCs. This result indicates that the Li^+ cation is not the origin of the difference between the dimer and monoporphyrin lifetimes. We note that the shorter lifetime values observed in Figure 4 with (electrolyte **II**) compared to those in Figure 3 (with electrolyte **I**) are likely due to the higher TiO_2 conduction band edge potential in the electrolyte without Li^+ as observed in previous studies,[37] and determined in this study from the V_{oc} vs electron density plots at matched electron density (Figure 5). A higher conduction band potential provides a larger excess free energy driving force for the recombination between TiO_2 electrons and the acceptor in the redox electrolyte, leading to increased recombination

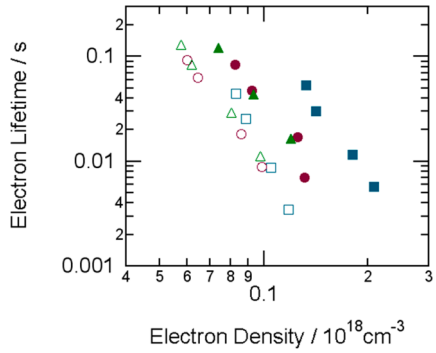

Figure 4. Electron lifetime vs electron density for DSSCs using **P199** (circles), **P12** (triangles), and **P10** (squares) with electrolyte II (closed) and electrolyte III (open).

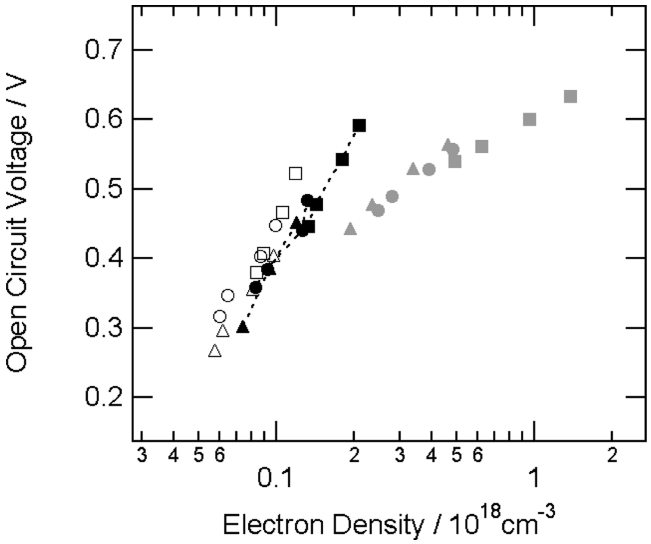

Figure 5. V_{oc} vs electron density for DSSCs using **P199** (circles), **P12** (triangles), and **P10** (squares) and containing electrolyte **Ib** (grey, closed) with electrolyte **II** (black, closed), and electrolyte **III** (open).

kinetics, and therefore a shorter electron lifetime. This negative conduction bands shift is also considered responsible for the significant reduction in the photocurrent observed from devices containing electrolytes **II** and **III** in comparison to those containing electrolyte **Ib**. The more negative conduction band reduces the overlap between the dye LUMO and the density of acceptor states in TiO_2, resulting in a reduced photocurrent.

Conversely, for devices prepared without tBP using electrolyte **III**, Figure 4 indicates that the lifetime of dimer DSSCs was comparable to that of the monomer DSSCs. Furthermore, a comparison between all dyes for devices containing electrolytes **II** (with tBP) and **III** (no tBP) shows that the electron lifetime of all dyes is improved in the presence of tBP. This improvement is most pronounced for the dimer molecule, leading to its longer lifetime in comparison to the monomer DSSCs. This observation implies that the presence of tBP in the electrolyte affects the dimer and monomer differently. We note that tBP molecule has recently been reported to interact with dye molecules.[38,39] One possible explanation for such an effect is an interaction of tBP molecules with the porphyrin dyes, creating a bulky dye structure. We have indeed observed a systematic red-shift in the absorption spectra of similar porphyrin dyes, named as GD2, as the concentration of tBP is increased (data not shown), implying their interactions. If the

tBP does indeed interact with the dye molecules for these sensitizers, then the bulky structure could then prevent the approach of I_3^- acceptor species to the TiO_2 surface. Since the dimer has multiple Zn atoms, this effect could be enhanced in comparison to the monoporphyrin dyes. Another effect could be that the coordination to the Zn atom would reduce the electrostatic force between the Zn cation and I_3^-.

To investigate whether the source of the dimer lifetime enhancement is a pure steric blocking affect (i), or whether partial charges (ii) or dispersion forces on the dye (iii) also influence the lifetime, measurements were performed at reduced dye loadings. A physical blocking effect is expected to be effective at high dye loadings and diminish largely at low dye surface coverage, whilst electrostatic or dispersive attraction forces decrease linearly with the amount of dyes. Therefore, at low dye surface coverages, parameters (ii) and (iii) are expected to be dominant in comparison to parameter (i). Accordingly, the concentration of monoporphyrin **P199** and dimer **P10** on the TiO_2 surface was therefore reduced by approximately 95% (referred to as "reduced" dye loading) of the dye coverage obtained under standard sensitization conditions (referred to as "full" dye-loading). This was achieved by decreasing the dye bath concentration and shortening the dye uptake time from 2 h to 30 min. When the dye loading of **P10** and **P199** was reduced, the electron lifetime became shorter for both dyes with respect to the 'full' coverage devices (Figure 3). This result is attributed to a more sparsely covered surface with lower packing density, which allows the approach of the I_3^- to the TiO_2 surface more readily. As seen for the "full" dye coverage devices, there were no major differences between the **P10** and **P199** devices in the D (Figure 3c) or the TiO_2 E_{CB} values (Figure 3d) at "reduced" surface loadings. Furthermore, there was no longer a difference observed in the electron lifetimes between the dimer and monomer-sensitized devices at these "reduced" dye loadings. This result supports that the longer electron lifetime observed for the **P10** "full" coverage devices is due to a steric blocking effect. The similar values of the lifetime at the reduced dye loading conditions suggests that the both dimer and monomer similarly attract acceptor species, implying no increase in dispersion force for the dimer.

One concern is if a change in the orientation of the dyes affects the above considerations. At full dye loading conditions, based on the measured amount of adsorbed dyes, the dimers are expected to be nearly orthogonal to the TiO_2 surface.[27] If the orientation of dimers changed to parallel to the TiO_2 surface at the reduced conditions, the concentration of porphyrin units near the surface would double, attracting more acceptor species and thus resulting in shorter electron lifetime in comparison to the case of the monomer under the same conditions and molar concentrations. Similarly, if the dimer exhibited larger attraction, e.g., dispersion, force and oriented more parallel to the TiO_2 surface, more acceptors at the vicinity of the TiO_2 surface would be expected. The similar observed lifetime values (and no increase in the attraction force) in Figure 4 imply that the dimer maintains its nearly orthogonal orientation even at reduced dye loading conditions.

Implications to the Strategy to Improve the Efficiency of Dye-Sensitized Solar Cells. To retard charge recombination in DSSCs, the local concentration of I_3^- at the TiO_2 surface should be minimized to reduce the probability of reverse charge transfer. This condition can be achieved by a careful consideration of the photosensitizer chemical structure. Dye molecules should ideally possess functional groups that enhance the blocking effect (i) and screen the electrostatic (ii) and dispersion forces (iii), since each of these conditions will reduce the amount of I_3^- attracted to the TiO_2 surface. In addition, it is often desirable to enlarge the dye molecules in order to extend the absorption spectrum onset into the infrared spectral region. However, this strategy can be problematic for maintaining low recombination rates because it also increases the undesirable dispersion forces due to the higher polarizability of the larger dye molecules. To maximize the blocking effect and dye absorption spectrum while preventing an increase in the dispersive forces, attaching sterically encumbering groups, which do not exhibit π-conjugation to the core dye structure, has been shown to be an effective approach.[40] The dimer molecule studied here also conforms to this design strategy in as much as the two porphyrin units do not maintain conjugation across both chromophores since they are oriented near-orthogonal to each other, as we have shown using computational modelling.[9] Thus, we have been able to introduce the blocking effect in dimer **P10** without increasing the dispersion forces of the molecule which attract I_3^- to the TiO_2 surface, leading to the observed increase in the electron lifetime of this dye. Coupled with improved light harvesting in the dimer-sensitized solar cells, these results indicate that the multichromophore approach without π conjugation among each unit presents a pathway towards further efficiency improvements in dye sensitized solar cells, providing a new strategy to design sensitizers with enhanced absorption coefficients without facilitating charge recombination in DSSCs.

CONCLUSIONS

Increased electron lifetime by one order of magnitude at matched electron density has been reported for a porphyrin dimer-sensitized TiO_2 solar cell in comparison to its monoporphyrin-sensitized analogue. This increase, which results in an improved open circuit voltage in operational devices, has been attributed to a steric blocking effect caused by the bulky dimer. This was evidenced by the decrease in the electron lifetime for the dimer at low dye surface concentrations. Furthermore, because the two porphyrin units are oriented orthogonal to each other, there is no overall increase in dispersion forces in the dimer which could counteract the steric blocking effect. The increased open circuit voltage is an additional benefit to the improved short circuit current produced by the enhanced light harvesting in the covalently linked porphyrin dimer, and suggests that the multichromophore dye approach without π conjugation among each unit can be used to further increase device efficiency by allowing enhanced light absorption without facilitating additional charge recombination.

ASSOCIATED CONTENT

Supporting Information

The change in V_{oc}, J_{sc}, and IPCE for monomer (**P199**) and dimer (**P10**) DSSCs sensitized using various dye bath concentrations and dye uptake times (Figures S1 and S2). The effect of chenodeoxycholic acid (CDCA) co-adsorber and a TiO_2 scattering layer on the electron diffusion coefficients, lifetime and the V_{oc} vs electron density plots for DSSCs sensitized with monomer **P12** and dimer **P10** (Figure S3). The effect of dye immersion time between 90 and 360 minutes on the electron diffusion coefficients, lifetime and the V_{oc} vs electron density plots for DSSCs sensitized with dimer **P10** (Figure S4). Current density–voltage curves measured under

AM 1.5 illumination and in the dark for DSSCs constructed without CDCA coadsorber and TiO_2 scattering layers using monomers **P199** and **P12**, and dimer **P10**. Values for current−voltage characteristics under one sun conditions (Table S1 and S2). This material is available free of charge via the Internet at http://pubs.acs.org

AUTHOR INFORMATION

Corresponding Authors

*E-mail: attila@uow.edu.au.
*E-mail: shogmori@shinshu-u.ac.jp.

Notes

The authors declare no competing financial interest.

ACKNOWLEDGMENTS

Financial support of the Australian Research Council through Centre of Excellence, Discovery and LIEF grants is acknowledged. A.J.M. is a recipient of an Australian Research Fellowship (DP110101369). Dr. R. Katoh and Dr. A. Furube are acknowledged for discussions.

REFERENCES

(1) O'Regan, B.; Grätzel, M. *Nature* **1991**, *353*, 737−740.
(2) Gregg, B. A.; Pichot, F.; Ferrere, S.; Fields, C. L. *J. Phys. Chem. B* **2001**, *105*, 1422−1429.
(3) Jennings, J. R.; Liu, Y.; Wang, Q.; Zakeeruddin, S. M.; Grätzel, M. *Phys. Chem. Chem. Phys.* **2011**, *13*, 6637−6648.
(4) Wiberg, J.; Marinado, T.; Hagberg, D. P.; Sun, L.; Hagfeldt, A.; Albinsson, B. *J. Phys. Chem. C* **2009**, *113*, 3881−3886.
(5) Mozer, A. J.; Wagner, P.; Officer, D. L.; Wallace, G. G.; Campbell, W. M.; Miyashita, M.; Sunahara, K.; Mori, S. *Chem. Commun.* **2008**, 4741−4753.
(6) Miyashita, M.; Sunahara, K.; Nishikawa, T.; Uemura, Y.; Koumura, N.; Hara, K.; Mori, A.; Abe, T.; Suzuki, E.; Mori, S. *J. Am. Chem. Soc.* **2008**, *130*, 17874−17881.
(7) O'Regan, B. C.; López-Duarte, I.; Martínez-Díaz, M. V.; Forneli, A.; Albero, J.; Morandeira, A.; Palomares, E.; Torres, T.; Durrant, J. R. *J. Am. Chem. Soc.* **2008**, *130*, 2906−2907.
(8) Marinado, T.; Nonomura, K.; Nissfolk, J.; Karlsson, M. K.; Hagberg, D. P.; Sun, L.; Mori, S.; Hagfeldt, A. *Langmuir* **2010**, *24*, 2592−2598.
(9) London, F. *Trans. Faraday Soc.* **1937**, *33*, 8b−26.
(10) Cameron, P. J.; Peter, L. M. *J. Phys. Chem. B* **2003**, *107*, 14394−14400.
(11) Allegrucci, A.; Lewcenko, N. A.; Mozer, A. J.; Dennany, L.; Wagner, P.; Officer, D. L.; Sunahara, K.; Mori, S.; Spiccia, L. *Energy Environ. Sci.* **2009**, *2*, 1069−1073.
(12) Feldt, S. M.; Cappel, U. B.; Johansson, E. M. J.; Boschloo, G.; Hagfeldt, A. *J. Phys. Chem. C* **2010**, *114*, 10551−10558.
(13) Neale, N. R.; Kopidakis, N.; van de Lagemaat, J.; Grätzel, M.; Frank, A. J. *J. Phys. Chem. B* **2005**, *109*, 23183−23189.
(14) Lee, K.-M.; Suryanarayanan, V.; Ho, K.-C.; Thomas, K. R. J.; Lin, J. T. *Sol. Ener. Mater. Sol. Cells* **2007**, *91*, 1426−1431.
(15) Wang, M.; Grätzel, C.; Moon, S.-J.; Humphry-Baker, R.; Rossier-Iten, N.; Zakeeruddin, S. M.; Grätzel, M. *Adv. Funct. Mater.* **2009**, *19*, 2163−2172.
(16) Zhang, Z.; Zakeeruddin, S. M.; O'Regan, B. C.; Humphry-Baker, R.; Grätzel, M. *J. Phys. Chem. B* **2005**, *109*, 21818−21824.
(17) Han, L.; Islam, A.; Chen, H.; Malapaka, C.; Chiranjeevi, B.; Zhang, S.; Yang, X.; Yanagida, M. *Energy Environ. Sci.* **2012**, *5*, 6057−6060.
(18) Koumura, N.; Wang, Z.-S.; Mori, S.; Miyashita, M.; Suzuki, E.; Hara, K. *J. Am. Chem. Soc.* **2006**, *128*, 14256−14257.
(19) Eu, S.; Katoh, T.; Umeyama, T.; Matano, Y.; Imahori, H. *Dalt. Trans.* **2008**, *40*, 5476−5483.
(20) Clifford, J. N.; Yahioglu, G.; Milgrom, L. R.; Durrant, J. R. *Chem. Commun.* **2002**, 1260−1261.
(21) Yella, A.; Lee, H.-W.; Tsao, H. N.; Yi, C.; Chandiran, A. K.; Nazeeruddin, M. K.; Diau, E. W.-G.; Yeh, C.-Y.; Zakeeruddin, S. M.; Grätzel, M. *Science* **2011**, *334*, 629−634.
(22) Warnan, J.; Pellegrin, Y.; Blarta, E.; Odobel, F. *Chem. Commun.* **2012**, *48*, 675−677.
(23) Park, J. K.; Chen, J.; Lee, H. R.; Park, S. W.; Shinokubo, H.; Osuka, A.; Kim, D. *J. Phys. Chem. C* **2009**, *113*, 21956−21963.
(24) Wu, H.-P.; Ou, Z.-W.; Pan, T.-Y.; Lan, C.-M.; Huang, W.-K.; Lee, H.-W.; Reddy, N. M.; Chen, C.-T.; Chao, W.-S.; Yeh, C.-Y.; Diau, E. W.-G. *Energy Environ. Sci.* **2012**, *5*, 9843−9848.
(25) Mai, C.-L.; Huang, W.-K.; Lu, H.-P.; Lee, C.-W.; Chiu, C.-L.; Liang, Y.-R.; Diau, E. W.-G.; Yeh, C.-Y. *Chem. Commun.* **2010**, *46*, 809−811.
(26) Liu, Y.; Lin, H.; Dy, J. T.; Tamaki, K.; Nakazaki, J.; Nakayama, D.; Uchida, S.; Kubo, T.; Segawa, H. *Chem. Commun.* **2011**, *47*, 4010−4012.
(27) Mozer, A. J.; Griffith, M. J.; Tsekouras, G.; Wagner, P.; Wallace, G. G.; Mori, S.; Sunahara, K.; Miyashita, M.; Earles, J. C.; Gordon, K. C.; Du, L.; Katoh, R.; Furube, A.; Officer, D. L. *J. Am. Chem. Soc.* **2009**, *131*, 15621−15623.
(28) Nakade, S.; Kanzaki, T.; Wada, Y.; Yanagida, S. *Langmuir* **2005**, *21*, 10803−10807.
(29) Duffy, N. W.; Peter, L. M.; Rajapakse, R. M. G.; Wijayantha, K. G. U. *Electrochem. Commun.* **2000**, *2*, 658−662.
(30) Peter, L. M.; Duffy, N. W.; Wang, R. L.; Wijayantha, K. G. U. *J. Electroanal. Chem.* **2002**, *524-525*, 127−136.
(31) Peter, L. *Acc. Chem. Res.* **2009**, *42*, 1839−1847.
(32) Nakade, S.; Kanzaki, T.; Kubo, W.; Kitamura, T.; Wada, Y.; Yanagida, S. *J. Phys. Chem. B* **2005**, *109*, 3480−3487.
(33) Kopidakis, N.; Benkstein, K. D.; van de Lagemaat, J.; Frank, A. J. *J. Phys. Chem. B* **2003**, *107*, 11307−11315.
(34) Yu, Q.; Wang, Y.; Yi, Z.; Zu, N.; Zhang, J.; Zhang, M.; Wang, P. *ACS Nano* **2010**, *4*, 6032−6038.
(35) Boschloo, G.l; Häggman, L.; Hagfeldt, A. *J. Phys. Chem. B* **2006**, *110*, 13144−13150.
(36) Kuang, D.; Klein, C.; Snaith, H. J.; Moser, J.-E.; Humphry-Baker, R.; Comte, P.; Zakeeruddin, S. M.; Grätzel, M. *Nano Lett.* **2006**, *6*, 769−773.
(37) Liu, Y.; Hagfeldt, A.; Xiao, X.-R.; Lindquist, S.-E. *Sol. Energy Mater. Sol. Cells* **1998**, *55*, 267−281.
(38) Gao, R.; Wang, L.; Geng, Y.; Ma, B.; Zhu, Y.; Dong, H.; Qiu, Y. *Phys. Chem. Chem. Phys.* **2011**, *13*, 10635−10640.
(39) Zhang, K.; Zhang, S.; Sodeyama, K.; Yang, X.; Chen, H.; Yanagida, M.; Tateyama, Y.; Han, L. *Appl. Phys. Expr.* **2012**, *5*, 042303−042305.
(40) Nishida, J.; Masuko, T.; Cui, Y.; Hara, K.; Shibuya, H.; Ihara, M.; Hosoyama, Y.; Goto, R.; Mori, S.; Yamashita, Y. *J. Phys. Chem. C* **2010**, *114*, 17920−17925.